Spitzer/IRS View of AGN Outflows

Barbara Medvar, Jack Gabel
Creighton University

Introduction

- We investigate how broad absorption line quasars (BALQSOs) compare to the normal quasar population using a sample of archival spectra obtained with the infrared spectrograph (IRS) aboard the *Spitzer Space Telescope*.
- BALs are detected in roughly 20% of the quasar population, yet it is unknown if this is due to:
  - Orientation: where BALs are present in all quasars, but detected in only a fraction due to a varied line-of-sight with respect to the anisotropic quasar geometry (e.g Gallagher et al. 2007, Hamann et al. 1993, Weymann et al. 1991) or
  - Evolution: where BALs represent a special evolutionary phase in the lifetime of the dynamic AGN quasar system (e.g Becker et al. 2000, and Canalizo & Stockton 2001; Voigt 1993).

- Here, we present results of a study comparing the mid-IR spectra of a sample of BALs and non-BALs and relating them to models from CLUMPY (Nenkova et al. 2002).

Sample Selection and Data

The key MIR diagnostics for our analysis are the broad Silicate dust band centered around 10μ and the MIR continuum slope.

- Thus, we selected BAL targets from the Spitzer/IRS database with z < 1 and full IRS wavelength coverage (~5-37μ, SL+LL) to sample the entire 10μ profile and best constrain the continuum shape.
- We identified 17 suitable BALs that meet our criteria from a search of the literature and Spitzer archival abstracts. We eliminated one outlier target from our sample, the ULIRG/ BAL Mrk 231, due to it's extreme rise in continuum flux from optical – MIR.
- To compare the BAL emission characteristics to the general quasar population, we also selected a control sample of PG quasars, chosen to have similar redshift and optical luminosities (Table 1).

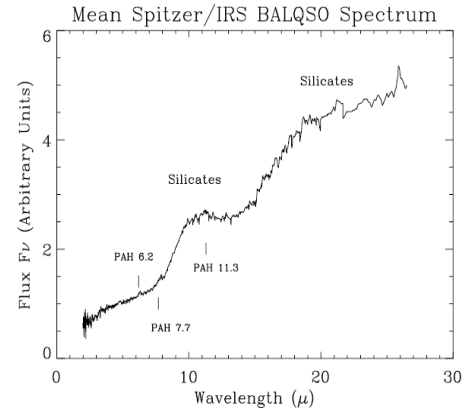

Fig 1: Average Spitzer/IRS spectra of the BALQSO sample (top) and control QSO sample (bottom). Individual spectra were shifted to rest wavelengths and normalized at 5 μ. The location of the Silicate bands and some typically prominent PAH emission features are Indicated.

Object	z	log L(.51μ)	log L(6.7μ)	L(6.7μ)/ L(.51μ)	17μm/6.7μm	Silicate Strength
BALQSO						
PG 0043+039	0.385	45.08	47.16	121.44	2.32	1.35 ± 0.06
IRAS 07598+6508	0.1483	45.22	46.35	13.44	2.01	0.21 ± 0.02
FIRST084044+363328	1.225		48.2		2.87	2.1 ± 0.3
PG 1004+130	0.24	44.98	46.8	65.97	1	2.1 ± 0.1
FIRST104459+365605	0.701	45.6	47.72	131.62	4.65	1.4 ± 0.3
PG 1254+047	1.02528		48.05		2.61	0.81 ± 0.04
PG 1351+640	0.0822	44.26	45.87	40.34	6.28	2.1 ± 0.1
PG 1535+547=Mrk 486	0.0389	43.59	45.18	39.33	1.898	0.4 ± 0.1
PG 1552+085	0.119	44.34	46.2	72.22	1.99	0.25 ± 0.01
FBQS J1558+3323	1.65424		48.62		1.69	0.19 ± 0.21
PG 1700+518	0.2899	45.4	46.96	36.03	3.13	0.07 ± 0.04
PG 2112+059	0.46005	45.32	47.31	98.6	2.36	0.25 ± 0.09
PHL1811	0.192	45.46	46.62	14.42	2.48	0.235 ± 0.004
QSO B2233+1328	0.325873		47.1		3.52	0.4 ± 0.1
LBQS 2359-1241	0.868	45.77	47.8	107.16	4.07	3.1 ± 0.3
IRAS 14026+4341	0.3233	45.37	47.07	49.91	3.45	0.47 ± 0.02
AVERAGE	**0.505**	**45.033**	**47.06**	**65.87**	**2.9 ± 1.3**	**1.0 ±0.1**
Control						
3C 454.3	0.859		47.96		3.11	0.08 ± 0.04
PG 0003+158	0.4509	45.33	47.39	114.83	3.55	1.1 ± 0.1
PG 0052+251	0.155	44.63	46.43	62.51	3.2	0.8 ± 0.1
PG 0921+525	0.035291	43.07	45.09	104.63	2.86	0.684 ± 0.005
PG 0953+414	0.2341	44.9	46.7	63.73	1.94	0.76 ± 0.07
PG 1022+519	0.044944	43.5	45.37	74.88	2.7	1.00 ± 0.2
PG 1049-005	0.3599	44.7	47.16	286.39	3.22	0.44 ± 0.07
PG 1116+215	0.1765	44.99	46.43	27.59	1.84	0.6 ± 0.1
PG 1259+593	0.4778	45.87	47.31	27.62	1.32	0.6 ± 0.06
PG 1309+355	0.184	44.4	46.62	164.71	4.09	1.0 ± 0.1
PG 1415+451	0.113587	44.2	46.16	90.36	2.83	0.5 ± 0.2
PG 1543+489	0.399609	45.19	47.43	175.76	3.41	0.1 ± 0.1
PG 1704+608	0.37194	44.87	47.12	177.61	3.79	0.74 ± 0.01
PG 1216+069	0.3313	45.17	47.04	74.72	1.68	0.48 ± 0.04
AVERAGE	**0.2996**	**44.68**	**46.73**	**111.18**	**2.8 ± 0.8**	**0.63 ± 0.09**

Table. 1. Col. (1): Object name. Col. (2): Redshift. Col. (3): Optical luminosity λL(5100 Å) rest wavelength. Col.(4): Infrared continuum luminosity λL at 6.7μ. Col(5): Luminosity ratio at 6.7 and .51μ. Col (6): MIR continuum slope as measured by flux ratio at 17 and 6.7μ. Including the standard deviation for the averages. Col.(6): Equivalent widths of the 10μ Silicate feature including each spectrum's calculated error.

CLUMPY Models of the Torus

- Since it is the most accepted theory at the moment, we assume that the torus is the dominating factor in the MIR spectra. It is also possible, however, that is from a Starburt or Extended NLR dust emission.
- We are looking in the infrared because a geometric change of the torus can make a significant difference in the spectrum. An example of this would be inclination angle (Figure 2) as shown by models from CLUMPY (Figure 2).
- CLUMPY models are the first to take into account the torus is made up of clumps of dusty matter rather than a smooth density torus (Nenkova et al. 2008).
- The user can create models by inputting the following parameters:
  - Ratio of outer to inner radii (Y)
  - Number of clouds in the radial direction (N)
  - Optical depth of a single cloud (τ)
  - Angular width of the torus (σ)
  - Power-law index of radial distribution (q)
- We determined default parameters for these models and determined the flux ratios as well as the equivalent widths for each inclination angle to compare to our Spitzer spectra.
- We also compared the models to each other varying each parameter to determine trends that occur in each parameter.

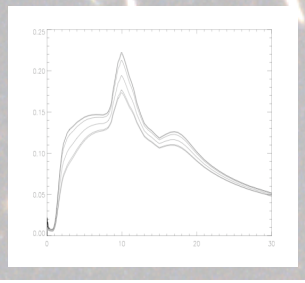

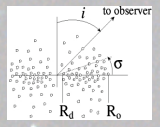

Fig. 2. (Top) The inclination angle is the angle at which we view the torus, measured from 0° looking down the center to 90° looking edge-on. A CLUMPY model (left) where the inclination angle is varied by 20° intervals from 0° on the top spectrum to 80° in the lowest spectrum shows significant changes to the 10μm bump as well as the continuum when the inclination angle is changed.

Results

- Comparing the strength of the Silicate bump, the MIR continuum slope, and the ratio of the luminosities for the BALQSOs versus the Control group, we can see that
  - Average Silicate strength for BALQSOs is ~40% larger than that of the Control QSOs.
  - MIR continuum slope is the same for both groups within about 1%
  - Ratio of Luminosities is approximately 41% smaller in the BALQSOs than in the Control QSOs.
- We statistically analyzed both groups using the Kolmogorov-Smirnov Test to determine if they two groups were from the same overall population..
- Results of the test:
  - For the 10μ Silicate bump: 18% chance they are from the same population (~1.3σ)
  - For the luminosity ratio: 23% chance they are from the same population (~1.1σ)
- Qualitatively, we found from analyzing the parameters for the CLUMPY models that the 10μ bump increases with the geometric parameters of the torus changing in this fashion:
  - Inclination angle → small
  - Y→ large
  - N→ small
  - τ → small
  - σ → small
  - q → 0 or 1

Conclusion and Discussion

-Not strong evidence for the torus geometric and emission parameters being different for our models
- No correlation between the torus inclination and the presence of a BAL
  - The disk wind model for AGN has a special orientation of the accretion disk relative to the observer's line of sight. If this is true, our data would imply the torus and the accretion disk are not aligned.
  - Additionally, our average 10 Silicate bump is larger for the BALs corresponding to a smaller inclination angle further contradicting the connection between the accretion disk and torus orientation in the context of disk wind model.
-A common evolution theory is that BALQSOs have more dusty material building up around them and thus get to a point where the material starts moving away in outflows. Since we cannot say our two groups are statistically different, our data does not support this theory (Voit et al. 1993).
  - Even if our two samples were statistically different, this evolution theory would imply that the BALQSOs had large toroidal structures around them that were thick and dense.
  - Relating this to the CLUMPY models, that would mean that Y, N, τ, and σ would all need to be large parameters while still having a large 10 μm bump which does not agree with our analysis.

In order to better this analysis and comparison in the MIR, more spectra need to be taken for BALQSOs.

References

Becker, R.H., et al., 2000, ApJ, 305, 83: Canalizo, G. & Stockton, A., ApJ, 555, 719; "CLUMPY" https://newt on.pa.uky.edu/~clumpyweb/; Gallagher, S. C., et al. 2007, ApJ, 665, 157; Hamann et al., 1993, ApJ, 415, 54; Nenkova, M., et al. 2002, ApJ, 570, L9-L12; Nenkova, M. et al. 2008 ApJ, 685, 147; NASA/IPAC Extragalaxtic Database (NED): http://nedwww.ipac.caltech.edu/; Netzer , H., et al. 2007, ApJ, 666, 806; Schweitzer, M., et al. 2008, ApJ, 679, 10; Spitzer Space Telescope http://archive.spitzer.caltech.edu/; Voit, G.M., 1993, ApJ, 413, 95; Weymann, R.J., et al. 1991, ApJ, 373, 23

Funding for this work has been provide by the NASA Nebraska Space Grant program. Special thanks to Todd Boroson for graciously providing optical spectra of the PG quasars. We acknowledge discussions with Nahum Arav that initially lead to this study.